THE JOURNAL OF BIOLOGICAL CHEMISTRY VOL. 290, NO. 35, pp. 21762–21772, August 28, 2015

Sickle Cell Hemoglobin with Mutation at αHis-50 Has Improved Solubility*

Received for publication, April 10, 2015, and in revised form, July 14, 2015 Published, JBC Papers in Press, July 16, 2015, DOI 10.1074/jbc.M115.658054

Ming F. Tam, Tsuey Chyi S. Tam, Virgil Simplaceanu, Nancy T. Ho, Ming Zou, and Chien Ho[1]

From the Department of Biological Sciences, Carnegie Mellon University, Pittsburgh, Pennsylvania 15213

Background: Deoxy sickle cell hemoglobin (Hb S) tetramers polymerize in solution via lateral and axial contacts among neighbors.
Results: αHis-50 → Gln mutation can, whereas αHis-20 → Gln mutation cannot, improve the solubility of Hb S.
Conclusion: α_2His-50 interacts with the $\beta^S{}_1$ CD corner, whereas α_2His-20 has minimal interaction with $\beta^S{}_1$Glu-22.
Significance: α_2His-50 contributes significantly to the polymerization of the Hb S tetramers.

The unliganded tetrameric Hb S has axial and lateral contacts with neighbors and can polymerize in solution. Novel recombinants of Hb S with single amino acid substitutions at the putative axial (recombinant Hb (rHb) (βE6V/αH20R) and rHb (βE6V/αH20Q)) or lateral (rHb (βE6V/αH50Q)) or double amino acid substitutions at both the putative axial and lateral (rHb (βE6V/αH20R/αH50Q) and rHb (βE6V/αH20Q/αH50Q)) contact sites were expressed in *Escherichia coli* and purified for structural and functional studies. The ^{1}H NMR spectra of the CO and deoxy forms of these mutants indicate that substitutions at either αHis-20 or αHis-50 do not change the subunit interfaces or the heme pockets of the proteins. The double mutants show only slight structural alteration in the β-heme pockets. All mutants have similar cooperativity (n_{50}), alkaline Bohr effect, and autoxidation rate as Hb S. The oxygen binding affinity (P_{50}) of the single mutants is comparable with that of Hb S. The double mutants bind oxygen with slightly higher affinity than Hb S under the acidic conditions. In high salt, rHb (βE6V/αH20R) is the only mutant that has a shorter delay time of polymerization and forms polymers more readily than Hb S with a dextran-Csat value of 1.86 ± 0.20 g/dl. Hb S, rHb (βE6V/αH20Q), rHb (βE6V/αH50Q), rHb (βE6V/αH20R/αH50Q), and rHb (βE6V/αH20Q/αH50Q) have dextran-Csat values of 2.95 ± 0.10, 3.04 ± 0.17, 11.78 ± 0.59, 7.11 ± 0.66, and 10.89 ± 0.83 g/dl, respectively. rHb (βE6V/αH20Q/αH50Q) is even more stable than Hb S under elevated temperature (60 °C).

Hb S[2] is a naturally occurring mutant of human adult hemoglobin (Hb A) that has the normally occurring glutamate at the β6 position of Hb A replaced with a valine (1). Heterozygous individuals carrying both Hb S and Hb A genes are protected against *Plasmodium* infection (2). However, homozygous individuals carrying only the Hb S genes develop hemolytic anemia (3, 4). The deoxygenated Hb S molecules form long fibers within the red blood cells, making them rigid and distorting them into the shape of a sickle. This leads to the blocking of capillary vessels and the destabilization of the red blood cell membranes and premature destruction of erythrocytes (5).

EM studies proposed that the Hb S fibers contain 14 (6) or 16 (7) individual strands twisted in a ropelike fashion. These strands can be arranged into seven or eight double strands, which are held together by inter-double strand, intra-double strand axial and intra-double strand lateral interactions (8, 9). The crystal structure of deoxy-Hb S has been determined (8, 10) and refined to 2.05 Å (11). In this paper, we adopt the designations of Padlan and Love (10, 12) in denoting the subunits of the tetramers in the double strands. The β-subunits that provide acceptor pockets for the βVal-6 are designated as $\beta^S{}_1$. The subunits that act as valine donors are assigned as $\beta^S{}_2$. The α-subunits are named according to the β-subunits with which they form dimers. According to the 2.05 Å structural model of Harrington *et al.* (11), each double strand is held together by the lateral interactions among $\beta^S{}_1$-subunits of one strand with the $\beta^S{}_2$- and α_2-subunits of tetramers from the other strand (Fig. 1*A*). The individual double strand is further stabilized by axial interactions between tetramers translated one unit cell along the vertical axis. The $\beta^S{}_1$-subunit of the lower tetramer makes contacts with the $\beta^S{}_2$- and the α_2-subunits of the upper tetramer. In addition, α_1- and α_2-subunit interactions are also present (Fig. 1*B*). The model gives a static picture of interacting amino acid residues that stabilize the polymer.

Numerous natural or recombinant Hb S mutants with substitution(s) at the putative contact sites have been selected or generated for studying the mechanism and inhibition of Hb S polymerization. The hydrophobicity and the size of the side chain of the amino acid at $\beta^S{}_2$6 or the $\beta^S{}_2$4 position affects the

* This work was supported, in whole or in part, by National Institutes of Health Grant R01GM084614. The authors declare that they have no conflicts of interest with the contents of this article.
[1] To whom correspondence should be addressed: Dept. of Biological Sciences, Carnegie Mellon University, 4400 Fifth Ave., Pittsburgh, PA 15213. Tel.: 412-268-3395; Fax: 412-268-7083; E-mail: chienho@andrew.cmu.edu.
[2] The abbreviations used are: Hb S, sickle cell hemoglobin, Hb A with βGlu-6 → Val (βE6V) mutation; Hb A, human adult hemoglobin; rHb, recombinant hemoglobin; rHb (βE6V/αH20R), recombinant sickle cell hemoglobin with additional αHis-20 → Arg mutation; rHb (βE6V/αH20Q), recombinant sickle cell hemoglobin with additional αHis-20 → Gln mutation; rHb (βE6V/αH50Q), recombinant sickle cell hemoglobin with additional αHis-50 → Gln mutation; rHb (βE6V/αH20R/αH50Q), recombinant sickle cell hemoglobin with additional αHis-20 → Arg and αHis-50 → Gln mutations; rHb (βE6V/αH20Q/αH50Q), recombinant sickle cell hemoglobin with additional αHis-20 → Gln and αHis-50 → Gln mutations; met-Hb, methemoglobin; HbCO, carbonmonoxy hemoglobin; P_{50}, partial O_2 pressure at 50% saturation; n_{50}, Hill coefficient at 50% O_2 saturation; Csat, solubility; t_d, delay time of polymerization; k_{auto}, autoxidation rate.

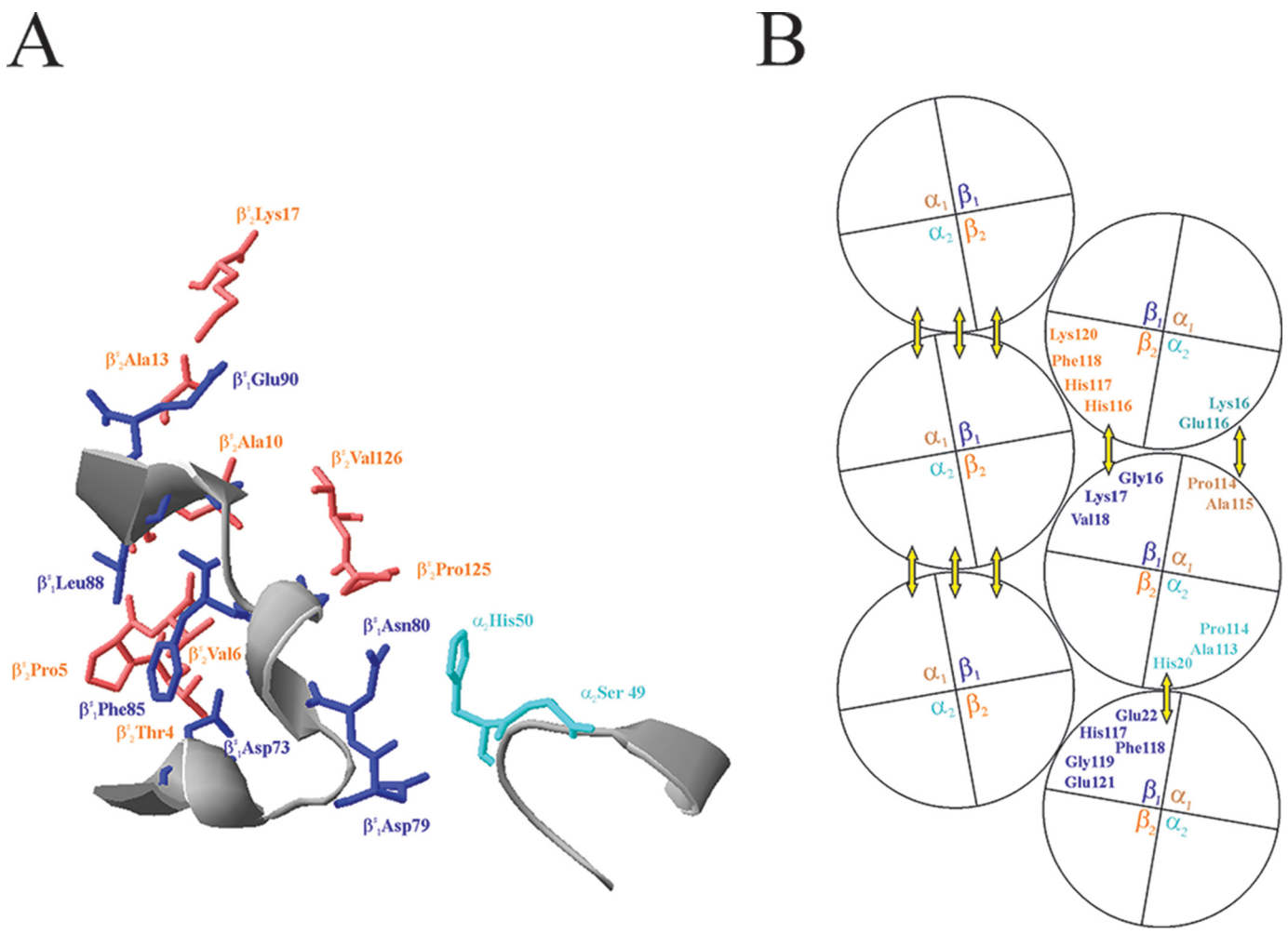

FIGURE 1. **Putative amino acid residues that participate in lateral (*A*) and axial contacts (*B*) in double strand Hb S polymers.** The lateral contacts are drawn according to coordinates in Protein Data Bank entry 2HBS. Residues from α_2-, $\beta^S{}_1$-, and $\beta^S{}_2$-subunits are *colored* in *cyan*, *blue*, and *coral*, respectively. The axial contacts are presented as in Ref. 8. The *yellow double arrows* depict the interacting subunits.

solubility of the resulting mutants (13–15). Solubility can be viewed as the concentration of hemoglobin that remains in solution after completion of polymerization. Mutations at the $\beta^S{}_1$ acceptor pocket can improve moderately the solubility of Hb S, but the mutants are inherently unstable (16–18). Himanen *et al.* replaced the βLys-95 at the acceptor pocket with Ile and disrupted one of the lateral contact sites (19, 20). The mutant is 2.6 times more soluble than Hb S under deoxy conditions (19). Sivaram *et al.* (21) removed one of the axial interactions by replacing the αLeu-113 with histidine and improved the Hb S solubility by 1.8 times. Mutants that carry a replacement at one of the axial contact sites and a substitution at the acceptor pocket (αP114R/βT87K and αH20Q/βT87Q) have improved solubility but still less than twice that of Hb S (22, 23).

The αHis-20 and the αHis-50 residues are located on the surface of the Hb S tetramer. The imidazole nitrogen of α_2His-20 is putatively in close proximity to the carboxyl side chain of $\beta^S{}_1$Glu-22 (11). A βE22Q mutant presumably disrupted part of the axial interactions between Hb S tetramers and showed a moderate increase (1.28-fold) in solubility (24). The α_2His-50 is postulated in lateral hydrogen-bonding distance from the $\beta^S{}_1$Asp-79 and the $\beta^S{}_1$Asn-80 side chains (11). Surprisingly, Hb S mutants with substitutions at this position have not been generated to study its effect on Hb S polymerization.

We report here the structural, functional, and polymerization properties of five recombinant Hb S mutants: rHb (βE6V/αH20R), rHb (βE6V/αH20Q), rHb (βE6V/αH50Q), rHb (βE6V/αH20R/αH50Q), and rHb (βE6V/αH20Q/αH50Q). We provide evidence that the putative axial interaction between αHis-20 and β^SGlu-22, as suggested by an x-ray crystallographic study, has minimal contribution in stabilizing the Hb S polymers. The solubility of Hb S can be improved markedly by replacing the αHis-50 with a glutamine. In particular, rHb (βE6V/αH50Q) and rHb (βE6V/αH20Q/αH50Q) are nearly 4 times more soluble than Hb S. Furthermore, rHb (βE6V/αH50Q) is more heat-stable than Hb S. To our knowledge, rHb (βE6V/αH50Q) is the most soluble Hb S mutant reported.

Experimental Procedures

Materials—Blood samples were obtained from the local blood bank (a normal human donor) and the National Institutes of Health (an Hb SS human donor) for the isolation of normal Hb A and Hb S, respectively. Restriction and related enzymes used in molecular biology work were purchased from New Eng-

land Biolabs. The QuikChange site-directed mutagenesis kit was a product from Stratagene. Chromatographic materials used in hemoglobin purification were obtained from GE Healthcare. Reagent grade chemicals were purchased from Sigma and used without further purification.

Recombinant Protein Expression and Purification—The expression vectors constructed in this study were derived from the pHE230 plasmid (22). The pHE230 plasmid encodes the *Escherichia coli* methionine aminopeptidase and synthetic human α- and β-globin genes under the control of separate *tac* promoters. The β-globin gene carries a βGlu-6 to valine substitution for the expression of recombinant Hb S proteins. The pHE230 was used as template in polymerase chain reactions to generate plasmids pHE295 (rHb (βE6V/αH20Q)), pHE2012 (rHb (βE6V/αH20R)), pHE296 (rHb (βE6V/αH50Q)), pHE297 (rHb (βE6V/αH20Q/αH50Q)), and pHE2022 (rHb (βE6V/αH20R/αH50Q)). The mutations on the plasmids were confirmed by DNA sequencing analysis of the entire α- and β-globin cDNAs.

The plasmids were transformed into JM109 cells for protein expression. Cells were grown in DM-4 medium (25) at 30 °C in a 20-liter fermenter (B. Braun Biotech International, model Biostat C). The induction and purification of rHb were carried out as described previously (26). Hb A and Hb S from whole blood were purified according to established methods in our laboratory (27, 28). Briefly, red blood cells were lysed with water and then loaded onto a Sephadex G-25 column equilibrated and eluted with 0.05 M Tris-HCl, pH 7.45, and 0.1 M NaCl. For the Hb S sample, it was further separated from other components by loading onto a Mono S column equilibrated with 10 mM phosphate, pH 6.8, and 0.5 mM EDTA. The column was developed with the 20 mM phosphate, pH 8.3, and 0.5 mM EDTA. Fractions corresponding to Hb S were collected. The Hb samples were then saturated with CO and stored frozen at −80 °C. The molecular weights of the Hb subunits were confirmed by mass spectrometry in an ion trap instrument equipped with an electrospray ionization source. The amount of N-terminal methionine cleavage of the samples was estimated by Edman degradation (26). All rHb samples in this study had the correct molecular weights and less than 5% unprocessed N-terminal methionine.

Oxygen Binding Properties—Oxygen dissociation curves were determined with a Hemox analyzer (TCS Medical Products) according to Shen *et al.* (26). The oxy-Hb samples at 0.1 mM Hb (in terms of heme) were prepared in 0.1 M sodium phosphate in the presence of catalase and superoxide dismutase to reduce the amount of met-Hb to less than 5% in all samples measured (29). Experiments were conducted at 29 °C as a function of pH. The experimental results were fit to the Adair equation using a nonlinear least-squares procedure. The partial pressure (in mm Hg) at 50% oxygenation (P_{50}) and the Hill coefficient (n_{50}) were determined from each curve. The experimental values had an accuracy of ±10% and S.D. values of ±4% between runs.

Dextran-Csat Assay and Polymerization Kinetic Measurements—Dextran-Csat assays were performed according to Tam *et al.* (28) for microsample handling. The polymerization progress curves were determined by the temperature-induced method of Adachi and Asakura (30) with modifications. Concentrated oxy-Hb sample (5–50 μl) was added to 3 ml of 1.8 M phosphate buffer, pH 7.4, and the solution was purged with nitrogen for 15 min. Sodium dithionite was then added to a final concentration of 10 mM, and the mixture was transferred to a sealed cuvette. The concentration of deoxy-Hb in the sample was determined by light absorbance at 555 nm and calculated by using a millimolar extinction coefficient ($mM^{-1}\ cm^{-1}$) of 12.5. The cuvette was chilled in ice water, and the temperature was monitored closely with a thermocouple. Once the temperature in the cuvette dropped to 2 °C, it was placed in a Cary 50 UV-visible spectrophotometer (Varian) with a cuvette holder preheated and maintained at 30 °C. Immediately, light absorbance at 700 nm, which reflects the turbidity of the sample, was recorded at 15-s intervals up to 2000 or 4000 s, depending on the polymerization speed of the sample. Routinely, the temperature of the sample increased from 2 to 30 °C in 325 s. The delay time of polyermerization (t_d) was determined from an A_{700} *versus* time plot according to Adachi and Asakura (30).

Autoxidation and Thermal Stability of rHb S Mutants—The autoxidation rate (k_{ox}) of the samples was determined as described (31). The concentration of oxy-Hb at each time point was calculated according to the equation, $[\text{Oxy-Hb}] = 0.2174A_{560} - 0.0573A_{577} - 0.1616A_{630}$ and expressed as a percentage of the original sample. The logarithm (base 10) of the percent oxy-Hb was plotted against time, and the slope of the plot gives the autoxidation rate. Thermal stability measurements were performed according to the outline of Adachi *et al.* (16). Briefly, oxygenated samples (50 μl, ~20 mg/ml) in 0.1 M sodium phosphate, pH 7.0, and 1 mM EDTA were aliquoted in quadruplicates into thin-walled polypropylene tubes and inserted into a GeneAmp PCR system 2700 (Applied Biosystems). The instrument was programmed to run at 60 °C for 10 min and then cooled to 25 °C in 1 min. The precipitates in the samples were removed by centrifugation, and the absorbance of the supernatants at 577 and 700 nm were recorded after appropriate dilution. The readings at 700 nm were treated as background and subtracted from the 577 nm readings. The background readings were less than 1% of the absorbance at 577 nm for the most diluted samples. Samples in triplicates without the heating step were used as controls, and the amount of precipitated proteins was calculated accordingly and expressed as a percentage.

Structural Study with ^1H NMR Spectroscopy—Proton NMR spectra of Hb A, Hb S, and its five mutants were obtained at 29 °C on Bruker Avance DRX-300 or DRX-600 spectrometers. Hb samples in carbonmonoxy form were concentrated to ~5% (3.1 mM in terms of heme) and exchanged into 0.1 M sodium phosphate at pH 7.0 in 95% water and 5% deuterium oxide (D_2O). Hb S and rHb mutants carrying a substitution at the αHis-50 position (rHb (βE6V/αH50Q), rHb (βE6V/αH20Q/αH50Q), and rHb (βE6V/αH20R/αH50Q)) were diluted to 2 and 4% solutions, respectively, before converting into the deoxy form for the NMR measurements. A jump-and-return pulse sequence was used to suppress the water signal (32).

TABLE 1

Oxygen binding properties and Bohr effect of Hb S and recombinant mutants

Experiments were conducted in 0.1 M sodium phosphate buffer at 29 °C in the presence of a methemoglobin reductase system (29). Values for the Bohr effect were estimated from the pH range in parentheses. Experiment results have an S.D. of <±4% between runs.

Hemoglobins	pH	P_{50}	n_{50}	$-\Delta(\log P_{50})/\Delta pH$
Hb A[a]	5.73	22.22	2.71	0.46 (pH 6.56–8.23)
	6.25	22.86	2.78	
	6.56	22.44	2.82	
	6.75	17.97	2.82	
	7.06	14.80	2.78	
	7.40	9.38	2.82	
	7.83	5.61	2.69	
	8.23	3.93	2.62	
Hb S	5.75	21.73	2.90	0.48 (pH 6.52–7.99)
	6.22	22.84	2.95	
	6.52	21.16	2.99	
	7.01	14.08	3.09	
	7.39	8.51	3.20	
	7.99	4.34	3.12	
rHb (βE6V/αH20Q)	5.82	20.98	2.61	0.45 (pH 6.51–8.23)
	6.26	21.91	2.73	
	6.51	19.38	2.68	
	7.02	13.13	2.78	
	7.40	7.79	2.90	
	7.71	5.49	2.93	
	8.23	3.34	2.90	
rHb (βE6V/αH20R)	5.80	21.61	2.81	0.48 (pH 6.51–8.10)
	6.27	22.50	2.88	
	6.51	21.14	2.98	
	6.97	13.63	2.85	
	7.39	8.48	3.06	
	8.10	3.75	2.99	
rHb (βE6V/αH50Q)	6.53	23.74	2.97	0.43 (pH 6.77–8.02)
	6.77	20.06	2.87	
	7.4	11.37	3.19	
	7.66	7.96	3.15	
	8.02	8.02	2.85	
rHb (βE6V/αH20R/H50Q)	5.74	16.41	2.47	0.45 (pH 6.49–7.98)
	6.19	18.40	2.58	
	6.49	16.41	2.58	
	7.02	10.99	2.76	
	7.38	6.93	2.93	
	7.98	3.63	2.83	
	8.62	2.81	2.78	
rHb (βE6V/αH20Q/H50Q)	5.76	16.85	2.62	0.46 (pH 6.52–8.00)
	6.22	18.61	2.68	
	6.52	17.08	2.68	
	7.03	11.48	2.78	
	7.41	7.07	2.81	
	8.00	3.70	2.69	
	8.70	2.60	2.57	

[a] Data from Tam *et al.* (31).

Results

Oxygen Binding and Cooperativity Properties of rHbs—The O_2 binding properties of Hb A, Hb S, and Hb S recombinant mutants with additional single (rHb (βE6V/αH20Q), rHb (βE6V/αH20R), and rHb (βE6V/αH50Q)) or double (rHb (βE6V/αH20Q/αH50Q) and rHb (βE6V/αH20R/αH50Q)) substitutions are summarized in Table 1. The αHis-20 and the αHis-50 are located on the surface of the tetramer (33). As expected, substitutions at these positions do not significantly change the O_2 binding properties of the macromolecules. The O_2 binding curves of the Hb S single mutants are essentially indistinguishable from that of Hb A or Hb S, whereas the Hb S double mutants have slightly higher O_2 binding affinity at low pH. The P_{50} values determined for the double mutants at acidic pH are ~20% lower than those of Hb S. All mutants in this study have Hill coefficients (n_{50}) of 2.5 or higher (Table 1). These results are indicative that these rHbs are cooperative in binding O_2.

Hemoglobin releases hydrogen ions upon oxygenation, and this alkaline Bohr effect can be expressed mathematically as $\Delta H^+ = -\Delta \log P_{50}/\Delta pH$ (34). The numbers of protons released per heme for Hb A, Hb S, and the recombinant mutants are listed in Table 1. The rHbs release 0.43–0.48 proton/heme, whereas Hb A and Hb S release 0.46 and 0.48 proton/heme, respectively. Hence, the mutants we generated are effective oxygen carriers.

Dextran-Csat and Polymerization Kinetic Measurements—The solubilities of Hb S and its recombinant mutants in the presence of dextran and low ionic strength buffer were determined according to the microassay of Tam *et al.* (28) and are listed in Table 2. Harrington *et al.* (11) estimated that in the double-stranded form of Hb S fibers, the imidazole nitrogen of the α_2His-20 is 3.55 Å from the side chain oxygen of $\beta^S{}_1$Glu-22 and suggested that they could form axial interaction. By eliminating the positive charge from the αHis-20, the rHb (βE6V/αH20Q) mutant has a Csat value of 3.04 ± 0.17 g/dl, which is close to that of Hb S (2.95 ± 0.10 g/dl). By elongating the side chain, the rHb (βE6V/αH20R) mutant apparently has improved interaction with neighboring tetramers, and the Csat value decreased to 1.86 ± 0.20 g/dl. These results imply that the interaction between the αHis-20 and the βGlu-22 of Hb S is minimal under dextran-Csat assay conditions at pH 7.5. In contrast, eradicating the positive charge from the αHis-50 position improves the solubility of the mutated rHb S. The rHb (βE6V/αH50Q) mutant has a Csat value of 11.78 ± 0.59 g/dl, which is 4 times higher than Hb S. This substitution can also improve the solubility of the rHb S mutated at the αHis-20 position. The rHb (βE6V/αH20R/αH50Q) mutant has a Csat value of 7.11 ± 0.66 g/dl, which is 3.8- and 2.4-fold higher than that of the rHb (βE6V/αH20R) mutant and Hb S, respectively. The rHb (βE6V/αH20Q/αH50Q) mutant has a Csat value of 10.89 ± 0.83 g/dl, which is ~3.6-fold higher than that of the rHb (βE6V/αH20Q) mutant and Hb S. Therefore, the solubility of Hb S can be improved by disrupting the lateral contacts between the α_2CD and the $\beta^S{}_1$EF corners.

The polymerization kinetics of the rHb S mutants was determined in 1.8 M phosphate buffer, pH 7.4, at 30 °C. The increase in turbidity of the sample, as measured by light scattering at 700 nm, reflects sample polymerization. The A_{700} values at various time points for each protein concentration can be plotted as a function of time to generate a sigmoidal curve. Some representative results for Hb S and its five mutants are presented in Fig. 2. The intercept of the slope at the *x* axis gave the delay time of polymerization (t_d). The delay time between the beginning of the experiment and the onset of polymerization depends on the initial hemoglobin concentration and increases as the protein concentration decreases. The logarithmic plots of the reciprocal of the delay time (t_d) *versus* the concentration of proteins are presented in Fig. 3 and summarize the data for multiple mutants at various concentrations for direct comparison. The plots for rHb (βE6V/αH20Q), rHb (βE6V/αH50Q), rHb (βE6V/αH20Q/αH50Q), and rHb (βE6V/αH20R/αH50Q) fall to the right of that representing Hb S. The results indicate that these mutants have longer polymerization delay time than Hb S. The plot for rHb (βE6V/αH20R) is shifted to the left of the plot for Hb S. The result suggests that rHb (βE6V/αH20R)

TABLE 2
Dextran-Csat value, autoxidation rate, and thermal stability of Hb S and recombinant mutants

	Dextran-Csat	Autoxidation rate	Thermal stability[a]
	g/dl	h^{-1}	
Hb A	ND[b]	0.00086 ± 0.0002	5.8 ± 0.1
Hb S	2.95 ± 0.10	0.0029 ± 0.0002	15.7 ± 0.2
rHb (βE6V/αH20R)	1.86 ± 0.20 2	0.0024 ± 0.0001	14.1 ± 0.2
rHb (βE6V/αH20Q)	3.04 ± 0.17	0.0023 ± 0.0002	13.9 ± 0.4
rHb (βE6V/αH50Q)	11.78 ± 0.59	0.0031 ± 0.0007	20.6 ± 1.0
rHb (βE6V/αH20R/αH50Q)	7.11 ± 0.66	0.0023 ± 0.0001	15.9 ± 0.9
rHb (βE6V/αH20Q/αH50Q)	10.89 ± 0.83	0.0025 ± 0.0002	12.0 ± 0.3

[a] Percentage denatured proteins after heating at 60 °C for 10 min.
[b] ND, not determined.

forms polymers faster than Hb S. Among these six plots in Fig. 3, only the line representing rHb (βE6V/αH20R) has a slope (1.91) significantly steeper than others (1.46–1.79). The slope of the line (*m*) is related to the size of the nucleus in forming aggregates (35, 36). Hence, the nuclei formed in the rHb (βE6V/αH20R) solution are larger than for Hb S and other mutants in this study.

Autoxidation and Thermal Stability—It has been suggested that Hb mutants have the potential to be used in gene therapy for sickle cell anemia (22). It is imperative to determinate the autoxidation rate (k_{ox}) and stability of the putative candidates. The successful candidate should have k_{ox} and stability similar to that of Hb S, if not Hb A. The k_{ox} of Hb A, Hb S, and its mutants were determined and are listed in Table 2. Hb S has a k_{ox} of 0.0029 ± 0.0002 h^{-1}, which is 3.4 times higher than that of Hb A (0.00086 ± 0.0002 h^{-1}). The Hb S mutants in this study all have substitution(s) on the protein surface and away from the heme pocket (33). Consequently, these mutants have k_{ox} ranging from 0.0023 to 0.0031 h^{-1}, very similar to that of Hb S.

Reportedly, oxy-Hb S was found mechanically (18) and thermally (16, 18) less stable than oxy-Hb A. We examined the thermal stability of the oxy form of Hb A, Hb S, and its mutants in a PCR thermal cycler, which has a more precise temperature control than in previous studies. Hb S has 15.7 ± 0.2% of denatured protein after heating at 60 °C for 10 min. Hb A has only 5.8 ± 0.1% denatured protein under the same experimental conditions. The results for the Hb S mutants are listed in Table 2. With the exception of rHb (βE6V/αH50Q), all mutants have thermal stability equal to or better than Hb S. In particular, rHb (βE6V/αH20Q/αH50Q) has only 12.0 ± 0.3% denatured protein under the same treatment, significantly better than Hb S. Apparently, Hb S mutants with substitution(s) on the protein surface are thermally more stable than Hb S with an additional mutation in the acceptor pocket (16, 18).

Structural Properties Investigated with ^1H NMR—The possible conformational changes of the rHb S mutants were investigated with ^{1}H NMR. αHis-122 and αHis-103 are located at the $\alpha_1\beta_1$ interface, and the $NH_{\epsilon 1}$ of their side chains give signals at 12.9 and 12.1 ppm, respectively (37–39). The exchangeable proton resonance spectra of the CO form of the samples show clearly that these two amino acid residues have not been disturbed in the five mutants studied (Fig. 4*A*).

βTrp-37 is located at the $\alpha_1\beta_2$ interface, and its $NH_{\epsilon 1}$ atom gives a resonance peak at 10.6 ppm (39, 40). As demonstrated in Fig. 4*A*, the resonances between 9.5 and 11.0 ppm are similar among Hb A, Hb S, and the five recombinant mutants. Therefore, substitutions at αHis-20 and αHis-50 do not change the quaternary structure of the liganded Hb A at the $\alpha_1\beta_2$ interface.

Resonances from 0 to −3 ppm belong to the non-exchangeable ring current-shifted protons, and they provide insight into the tertiary structure of the heme pockets. The γ_2-CH_3 groups of αVal-62 and βVal-67 of the distal heme pocket give resonances at −1.75 and −1.82 ppm relative to 2,2-dimethyl-2-silapentanesulfonic acid, respectively (41, 42). The signals at −1.75 ppm are similar among all six proteins studied. However, the signal at −1.82 ppm is shifted slightly upfield for the rHb (βE6V/αH20R/αH50Q) and the rHb (βE6V/αH20Q/αH50Q) mutants, although the mutations are on the α-subunit (Fig. 4*B*). Moreover, the resonances between −0.7 and −1.1 ppm for the double mutants differ significantly from those for the other five proteins. But, we have not yet assigned the resonances for these signals and cannot comment on their importance.

The ^{1}H NMR spectra for the deoxy form of Hb A, Hb S, rHb (βE6V/αH50Q), rHb (βE6V/αH20R/αH50Q), and rHb (βE6V/αH20Q/αH50Q) are presented in Fig. 5. The deoxy forms of Hb S mutants with a single substitution at αHis-20 are at least 3-fold less soluble than mutants carrying a substitution at the αHis-50 position, and they were excluded from the NMR experiments. The hyperfine-shifted proton resonances of the $N_\delta H$ exchangeable proton of αHis-87 and βHis-92 in the proximal heme pocket appear at 63 and 76 ppm from 2,2-dimethyl-2-silapentanesulfonic acid, respectively (43, 44). The signals for the mutants, Hb S, and Hb A appear at the same positions (Fig. 5*A*).

Fig. 5*B* presents the spectral region of the deoxy form of the proteins between 11 and 25 ppm downfield from 2,2-dimethyl-2-silapentanesulfonic acid. The porphyrin rings of the α- and β-subunits resonate at 17.0 and 22.6 ppm, respectively (45). The signals at 14.1 and 11.2 ppm have been assigned to the hydrogen bonds between αTyr-42 and βAsp-99 and between βTrp-37 and αAsp-94, respectively. These residues are located in the $\alpha_1\beta_2$ interface, and the resonances are important T-state markers of the deoxy-Hb A (39, 46, 47). We did not detect any difference in chemical shift for these signals among the five proteins. The signals at 12.9 and 12.1 ppm belong to αHis-122 and αHis-103, as in the spectra for the liganded form of the molecules. Again, we cannot detect any shift in the signals for the mutants.

In summary, the β-heme pockets of the liganded form of rHb (βE6V/αH20R/αH50Q) and rHb (βE6V/αH20Q/αH50Q) changed slightly when compared with that of Hb A or Hb S.

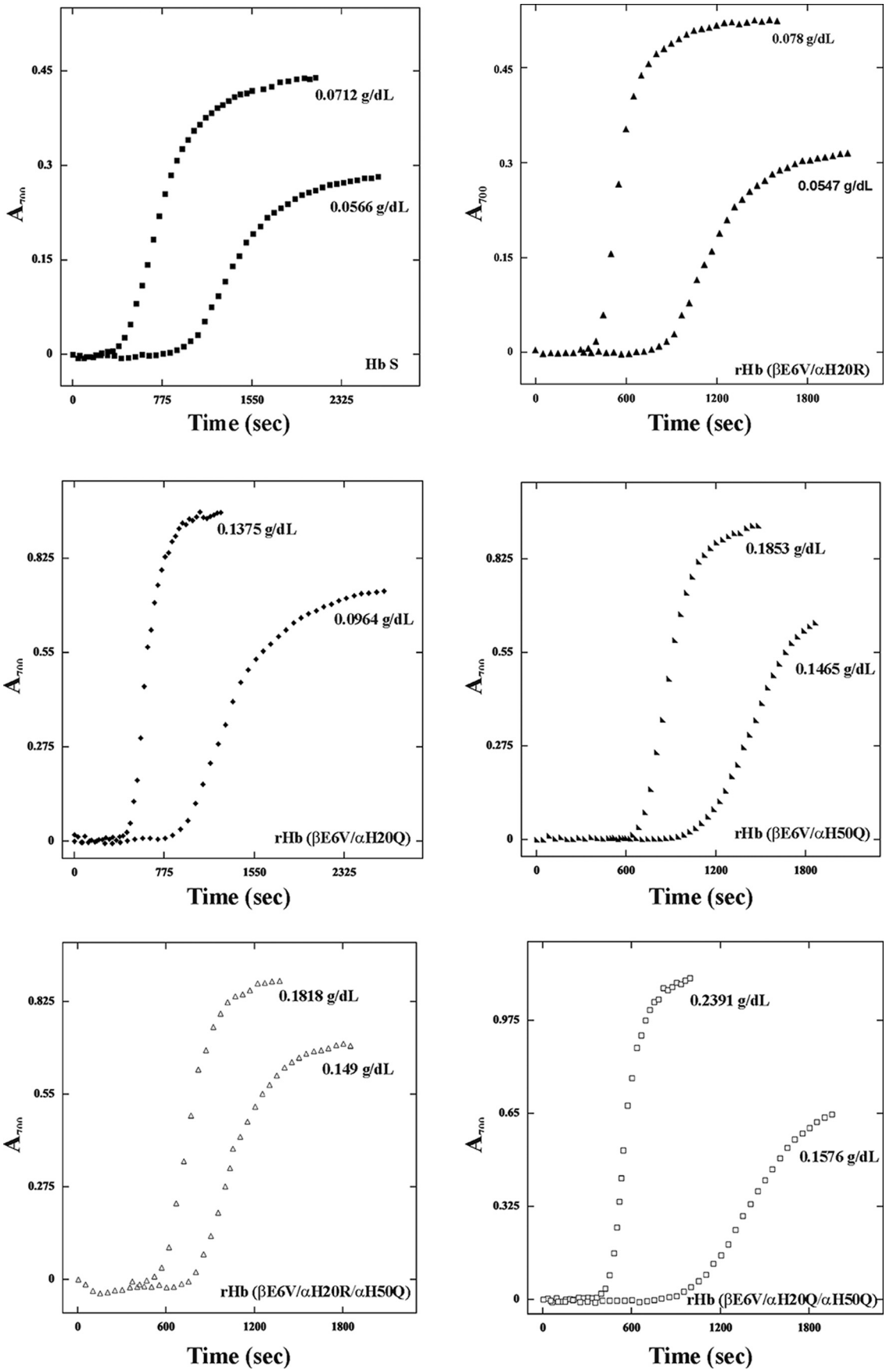

FIGURE 2. **Polymerization of Hb S and its recombinant mutants.** Polymer formation was assessed by light scattering at 700 nm in 1.8 M phosphate buffer at pH 7.4. Data are presented for each protein at two different concentrations. The *scales* on the *x* and *y* axis vary among the *panels*.

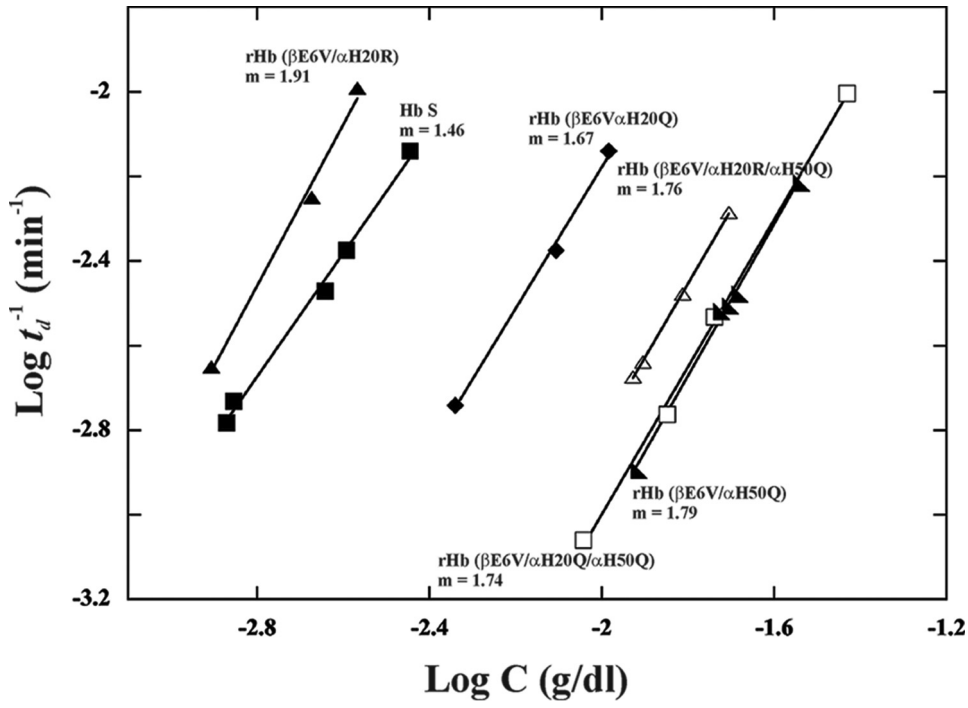

FIGURE 3. **Kinetics of polymerization of Hb S and its recombinant mutants in concentrated phosphate buffer.** The log values of the reciprocal of the delay times of polymerization are plotted against the log of hemoglobin concentrations. The slopes (*m*) of the plots are indicated.

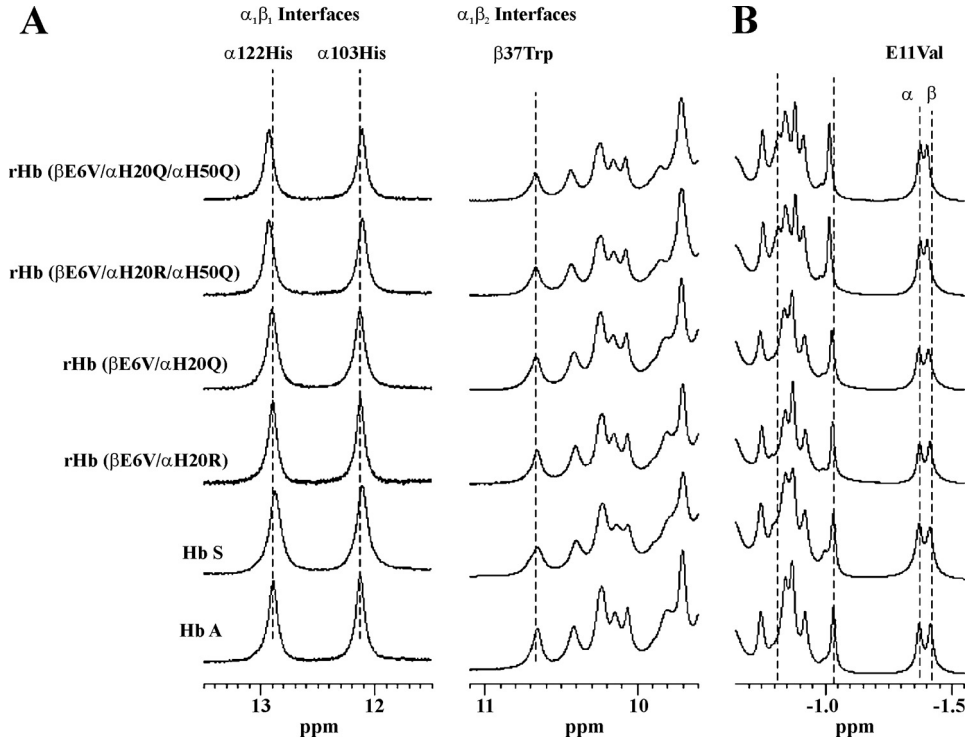

FIGURE 4. **^{1}H NMR spectra of the CO form of Hb A, Hb S, and rHbs.** Spectra of exchangeable proton resonances (*A*) and ring current-shifted proton resonances (*B*) were acquired at 600 MHz in 95% H_2O, 5% D_2O, and 0.1 M sodium phosphate buffer at pH 7.0 and 29 °C.

Besides that, the tertiary and quaternary structures of the four mutants are similar to that of Hb A or Hb S.

Discussion

The oxy forms of Hb A and Hb S have similar solubility. Upon deoxygenation, the solubility of Hb A was decreased by half, whereas that of Hb S diminished by 100 times (48). The primary sequences of Hb S and Hb A differ in a single amino acid. Hb S has a hydrophobic valine instead of a hydrophilic glutamic acid at the β6 position. Furthermore, mutants with isoleucine (49) and lysine (13, 50) at the β6 position have lower and higher solubility, respectively, than Hb S. There-

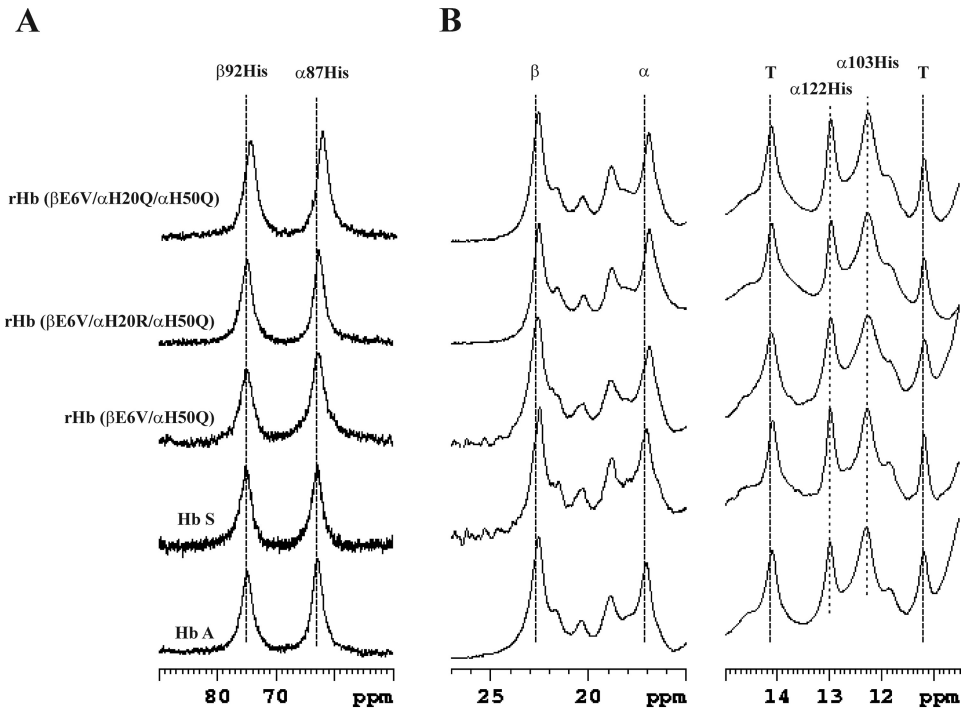

FIGURE 5. **^{1}H NMR spectra of the deoxy form of Hb A, Hb S, and rHbs.** Spectra of the hyperfine-shifted $N_\delta H$ proton resonances of the proximal histidyl residues (*A*) and the hyperfine-shifted and exchangeable proton resonances (*B*) were acquired at 300 MHz in 95% H_2O, 5% D_2O, and 0.1 M sodium phosphate buffer at pH 7.0 and 29 °C.

fore, lowering solubility and forming polymers can be attributed to this single amino acid substitution, a direct result of introducing undesirable interactions among surface residues of neighboring tetramers.

We have generated five Hb S mutants for this study. Three of them carry an additional substitution at the α20 or the α50 position (rHb (βE6V/αH20R), rHb (βE6V/αH20Q), and rHb (βE6V/αH50Q)), whereas the other two carry mutations at both α20 and α50 positions (rHb (βE6V/αH20R/αH50Q) and rHb (βE6V/αH20Q/αH50Q)). These Hb S mutants have substituted amino acid(s) on the surface of the tetrameric protein and away from the heme pockets and the $\alpha_1\beta_1$ and the $\alpha_1\beta_2$ interfaces. Hence, these mutants are structurally (Figs. 4 and 5) and functionally (Fig. 2 and Tables 1 and 2) similar to Hb S. Their autoxidation rate is similar to that of Hb S. For some mutants (rHb (βE6V/αH20Q), rHb (βE6V/αH20Q), and rHb (βE6V/αH20Q/αH50Q), they are thermally more stable than Hb S.

EM studies (6, 51) indicate that the double strands within the Hb S fibers have a slight helical twist. The results give an overall conformation of the fiber but cannot pinpoint the interacting residues with certainty. Data from x-ray crystallography have higher resolution, but the double strands found in the Hb S crystals are straight and do not have the helical twist (10–12).

Harrington *et al.* (11) refined the crystal structure of deoxy-Hb S to 2.05 Å and then employed the program CONTACT to identify inter- and intrastrand interacting residues. With this approach, 34 residues from the β_1/β_2-subunits and 9 residues from the α_1/α_2-subunits are suggested to be within interacting distances either laterally or axially among Hb S tetramers. These putative interacting residues are listed in Table 3.

According to the model of Harrington *et al.* (11), the axial contacts can be grouped as follows: (i) the GH corner (α_1Pro-114 and α_1Ala-115) of the α_1-subunit of the lower tetramer interacts with the GH corner (α_2Glu-116) and A helix (α_2Lys-16) of the α_2-subunit of the upper tetramer; (ii) the A helix ($\beta^S{}_1$Gly-16, $\beta^S{}_1$Lys-17, and $\beta^S{}_1$Val-18) of the $\beta^S{}_1$-subunit of the lower tetramer interacts with the G helix ($\beta^S{}_2$His-116 and $\beta^S{}_2$His-117) and the GH corner ($\beta^S{}_2$Phe-118 and $\beta^S{}_2$Lys-120) of the $\beta^S{}_2$-subunit of the upper tetramer; (iii) the G helix ($\beta^S{}_1$His-117) and the GH corner ($\beta^S{}_1$Phe-118, $\beta^S{}_1$Gly-119, and $\beta^S{}_1$Glu-121) of the $\beta^S{}_1$-subunit of the lower tetramer interacts with the GH corner (α_2Pro-114 and α_2Ala-115) of the α_2-subunit of the upper tetramer; and (iv) the B helix ($\beta^S{}_1$Glu-22) of the $\beta^S{}_1$-subunit of the lower tetramer interacts with the B helix (α_2His-20) of the α_2-subunit of the upper tetramer. These interacting residues are presented as a diagram in Fig. 1*B*. Because the coordinates in the Protein Data Bank file 2HBS cannot pinpoint the relative positions of the interacting residues, we summarized the interacting residues as did Wishner *et al.* (8).

The lateral interactions contributing to the Hb S polymerization are mainly between $\beta^S{}_1$ of one strand and the $\beta^S{}_2$ of the neighboring strand. Seven residues from the A helix, including the substituted βVal-6, plus two residues from the H helix of $\beta^S{}_2$ interact with 13 residues from the E and F helices and the EF and FG corners of the neighboring $\beta^S{}_1$-subunit (Table 3 and Fig. 1*A*). The interactions between the $\beta^S{}_1$ EF corner (βAsp-79 and βAsn-80) and the α_2 CD corner (αSer-49 and αHis-50) constitute the only lateral contact between β^S- and α-subunits. In particular, the side chains of $\beta^S{}_1$Asp-79 and α_2His-50 are reportedly separated by only 2.83 Å (11). However, according to the deposited coordinates (Protein Data Bank code 2HBS) of

TABLE 3

Putative amino acid residues that participate in lateral and axial contacts in double strand Hb S polymers (11)

Interacting residues are highlighted with the same color or connected with double-headed arrows.

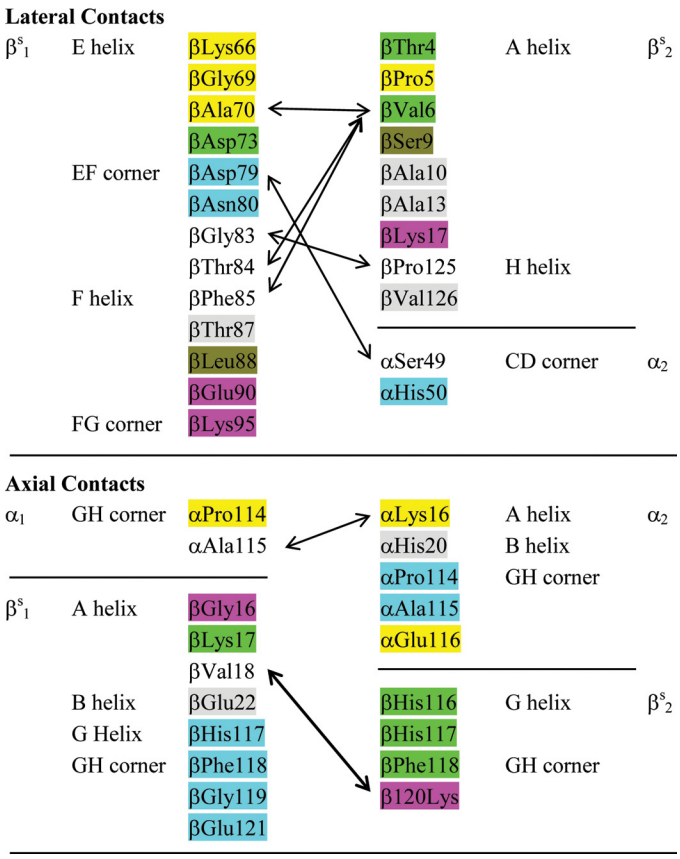

the two Hb S tetramers in the unit cell, the imidazole nitrogen of α_2His-50 is 6 Å from the side chain oxygen of $\beta^S{}_1$Asp-79. The distance between the side chains of α_2His-50 and $\beta^S{}_1$Asn-80 is shorter (3.86 Å) but still too far for hydrogen bonding. Therefore, these results generated from docking calculations should be confirmed with biochemical and mutagenesis studies.

Careful scrutiny of the docking results reveals that only five (αLys-16, αHis-20, αPro-114, αAla-115, and αGlu-116) and two (αSer-49 and αHis-50) residues on the α-subunits contribute to either axial or lateral interactions, respectively. Russu and Ho (52) have suggested the presence of histidyl residues at contact areas between Hb S molecules in pregelation aggregates. Therefore, αHis-20 and αHis-50, the only two histidines among the list, were selected for mutation, and its effect on Hb S solubility was studied.

Presumably, α_2His-20 and $\beta^S{}_1$Glu-22 form an interacting pair in the Hb S fibers. Nagel *et al.* (53) compared the β and γ sequences of the hemoglobin subunit and determined the minimum gelling concentration of a mixture of Hb S and Hb G Coushatta (βGlu-22 → Ala). They suggested that β^SGlu-22 possibly partially stabilized the deoxy-Hb S polymers. Acharya and Seetharam (54) modified the β^SGlu-22 and the β^SGlu-43 with glucosamine, and they observed an increase in the solubility of the modified deoxy-Hb S by about 55%. However, the addition of glucosamine not only eliminated the carboxyl side chain of β^SGlu-22 but appended also a bulky carbohydrate derivative that might interfere with subunit-subunit interactions. Therefore, whether disrupting the putative α_2His-20 and $\beta^S{}_1$Glu-22 interaction can improve Hb S solubility is debatable.

Hb S carrying mutations at the α20 position have been studied (23, 24, 55). Rhonda *et al.* (55) measured the solubility of an equal mixture of Hb S and Hb Le Lamentin (Hb S with an αHis-20 → Gln mutation) and claimed a 1.6-fold increase in Csat value. Srinivasulu *et al.* (23) measured the solubility of Hb Le Lamentin with an oxygen affinity method and reported only a 26% increase in Csat. Banerjee *et al.* (24) used the dextran-Csat method of Bookchin *et al.* (56) and reported a 28% increase in Csat value for the same mutant.

We used the dextran-Csat method of Tam *et al.* (28) developed for microsample handling in this study. Our Hb Le Lamentin (rHb (βE6V/αH20Q)) has a Csat value similar to that of Hb S without any pronounced improvement (Table 2), although the polymers formed more slowly than for Hb S (Fig. 3). The 3.55-Å distance (11) between the $N_{\epsilon 2}$ atom of the α_2His-20 and the $O_{\epsilon 2}$ atom of the β_1Glu-22 is possibly too long for optimal hydrogen bond formation. However, the structure of Hb in solution is flexible, and its backbone and side chains can exhibit various types of motions (see Ref. 57 for a review). Hence, it is conceivable that a subpopulation of the Hb possibly assumes a conformation with a shorter distance between α_2His-20 and β_1Glu-22 for hydrogen bonding. The conservative substitution of Gln for His at the α20 position disrupts this interaction and abolished the contribution of α_2His-20 and β_1Glu-22 to the polymerization process, resulting in a lengthening in the delay time of polymerization.

To further explore the possible interaction between α_2His-20 and $\beta^S{}_1$Glu-22, we generated the rHb (βE6V/αH20R) mutant. rHb (βE6V/αH20R) has a Csat value of 1.86 ± 0.20 g/dl (Table 2), which is only two-thirds of that of Hb S. It has also a shorter delay time of polymerization, and the size of nucleus in forming aggregates is larger than for Hb S (Fig. 3). Hence, the interactions between neighboring Hb S tetramers are intensified by introducing a longer side chain carrying a positive charge at the α20 position. Adachi *et al.* (58) have investigated the polymerization of Hb S in the presence of Hb A_2 variants carrying Val, Glu, and Thr at positions 6, 22, and 87 of the δ-subunit. They concluded also that it is not necessary to change Glu to Ala at the β22 position in preparing anti-sickling hemoglobin. Therefore, we conclude that the interaction between α_2His-20 and $\beta^S{}_1$Glu-22 contributes minimally to the polymerization of Hb S.

The lateral interactions among residues on the $\beta^S{}_2$-subunit with the neighboring $\beta^S{}_1$ EF pocket have been studied extensively. For instance, mutants with an aromatic residue (phenylalanine or tryptophan) at the β6 position are more soluble than Hb S (59). Probably, it is more difficult to insert a bulky side chain into the EF pocket. The observation that the rHb (βE6V/βL88F) mutant, with an aromatic residue in the EF pocket, also has higher solubility substantiates this speculation (16). Other residues on or near the acceptor site have also been mutated to disrupt the lateral interactions in various studies. In general, the mutants have moderately improved solubility (16, 18, 19, 22, 60,

61), but some of them reportedly suffered from thermal instability (16, 18, 61).

According to the model proposed by Harrington *et al.* (11), $\beta^S{}_1$Asp-79 interacts with both α_2Ser-49 and α_2His-50, whereas $\beta^S{}_1$Asn-80 interacts only with α_2His-50. Nagel *et al.* (53) have investigated the solubility of Hb S in the presence of an Hb A_2 mutant containing a βAsn-80 → Lys mutation and observed a 19% increase in solubility. McCune *et al.* (62) generated an Hb S mutant with the addition of βGlu-22 → Ala and βAsn-80 → Lys substitutions. This mutant is better than Hb A but less effective than Hb F in inhibiting the polymerization of Hb S. Srinivasulu *et al.* (63) substituted the αSer-49 on Hb S with Arg and observed a 60% increase in solubility. However, the contribution of α_2His-50 in stabilizing the Hb S polymer has never been tested.

To address this issue, we generated the rHb (βE6V/αH50Q) mutant, which has a Csat value 4 times higher than that of Hb S (Table 2). The results show clearly that removing the positive charge on αHis-50 interrupts its interaction with the neighboring $\beta^S{}_1$Asp-79 and/or $\beta^S{}_1$Asn-80. Furthermore, this substitution at the αHis-50 position also improves the solubility of rHb (βE6V/αH20R) and rHb (βE6V/αH20Q). The resulting rHb (βE6V/αH20Q/αH50Q) mutant has a dextran-Csat value of 10.89 ± 0.80 g/dl, which is 3.7 times higher than Hb S. It has similar autoxidation rate and better thermal stability than Hb S (Table 2). The rHb (βE6V/αH20R/αH50Q) mutant has a dextran-Csat value of 7.11 ± 0.66 g/dl (Table 2), which is 3.8 times better than that of the rHb (βE6V/αH20R) mutant. Both mutants have a longer delay time of polymerization compared with that of Hb S (Fig. 3). Furthermore, the results also suggest that the effects of mutation at positions α20 and α50 are independent of each other.

In summary, the results in this report show that (i) the interaction between α_2His-20 and $\beta^S{}_1$Glu-22 is minimal in stabilizing the Hb S polymer, and (ii) the Hb S polymer can be destabilized by replacing the histidyl residue at the α50 position with a Gln. The resulting protein is functionally and structurally similar to Hb S. The mutant carrying the αHis-50 → Gln substitution can be a candidate for gene therapy of sickle cell disease.

Author Contributions—M. F. T. and C. H. designed the study and wrote the paper. T. C. S. T. purified all of the samples in this study and performed and analyzed the experiments in Table 2. V. S. collected and analyzed all NMR spectra. N. T. C. performed and analyzed the experiments shown in Table 1. M. Z. performed and analyzed the experiments shown in Figs. 2 and 3. All authors reviewed the results and approved the final version of the manuscript.

Acknowledgment—We thank Dr. Chwan-Deng Hsiao (Academia Sinica) for helpful discussion on the crystal structure of Hb S.

References

1. Ingram, V. M. (1959) Abnormal human haemoglobins. III. The chemical difference between normal and sickle cell haemoglobins. *Biochim. Biophys. Acta* **36,** 402–411
2. Williams, T. N. (2006) Human red blood cell polymorphisms and malaria. *Curr. Opin. Microbiol.* **9,** 388–394
3. Eaton, W. A., and Hofrichter, J. (1987) Hemoglobin S gelation and sickle cell disease. *Blood* **70,** 1245–1266
4. Reiter, C. D., Wang, X., Tanus-Santos, J. E., Hogg, N., Cannon, R. O., 3rd, Schechter, A. N., and Gladwin, M. T. (2002) Cell-free hemoglobin limits nitric oxide bioavailability in sickle-cell disease. *Nat. Med.* **8,** 1383–1389
5. Bensinger, T. A., and Gillette, P. N. (1974) Hemolysis in sickle cell disease. *Arch. Intern. Med.* **133,** 624–631
6. Dykes, G. W., Crepeau, R. H., and Edelstein, S. J. (1979) Three-dimensional reconstruction of the 14-filament fibers of hemoglobin S. *J. Mol. Biol.* **130,** 451–472
7. Wellems, T. E., and Josephs, R. (1979) Crystallization of deoxyhemoglobin S by fiber alignment and fusion. *J. Mol. Biol.* **135,** 651–674
8. Wishner, B. C., Ward, K. B., Lattman, E. E., and Love, W. E. (1975) Crystal structure of sickle-cell deoxyhemoglobin at 5 Å resolution. *J. Mol. Biol.* **98,** 179–194
9. Watowich, S. J., Gross, L. J., and Josephs, R. (1989) Intermolecular contacts within sickle hemoglobin fibers. *J. Mol. Biol.* **209,** 821–828
10. Padlan, E. A., and Love, W. E. (1985) Refined crystal structure of deoxyhemoglobin S. II. Molecular interactions in the crystal. *J. Biol. Chem.* **260,** 8280–8291
11. Harrington, D. J., Adachi, K., and Royer, W. E., Jr. (1997) The high resolution crystal structure of deoxyhemoglobin S. *J. Mol. Biol.* **272,** 398–407
12. Padlan, E. A., and Love, W. E. (1985) Refined crystal structure of deoxyhemoglobin S. I. Restrained least-squares refinement at 3.0-Å resolution. *J. Biol. Chem.* **260,** 8272–8279
13. Adachi, K., Kim, J., Travitz, R., Harano, T., and Asakura, T. (1987) Effect of amino acid at the β6 position on surface hydrophobicity, stability, solubility, and the kinetics of polymerization of hemoglobin. Comparisons among Hb A (Glu β6), Hb C (Lys β6), Hb Machida (Gln β6), and Hb S (Val β6). *J. Biol. Chem.* **262,** 12920–12925
14. Adachi, K., Ding, M., Asakura, T., and Surrey, S. (2009) Relationship between β4 hydrogen bond and β6 hydrophobic interactions during aggregate, fiber or crystal formation in oversaturated solutions of hemoglobin A and S. *Arch. Biochem. Biophys.* **481,** 137–144
15. Adachi, K., Ding, M., and Surrey, S. (2008) Role of the β4Thr-β73Asp hydrogen bond in HbS polymer and domain formation from multinucleate-containing clusters. *Biochemistry* **47,** 5441–5449
16. Adachi, K., Konitzer, P., Paulraj, C. G., and Surrey, S. (1994) Role of Leu-β88 in the hydrophobic acceptor pocket for Val-β6 during hemoglobin S polymerization. *J. Biol. Chem.* **269,** 17477–17480
17. Adachi, K., Konitzer, P., and Surrey, S. (1994) Role of γ87 Gln in the inhibition of hemoglobin S polymerization by hemoglobin F. *J. Biol. Chem.* **269,** 9562–9567
18. Adachi, K., Reddy, L. R., and Surrey, S. (1994) Role of hydrophobicity of phenylalanine β85 and leucine β88 in the acceptor pocket for valine β6 during hemoglobin S polymerization. *J. Biol. Chem.* **269,** 31563–31566
19. Himanen, J.-P., Popowicz, A. M., and Manning, J. M. (1997) Recombinant sickle hemoglobin containing a lysine substitution at Asp-85(α): expression in yeast, functional properties, and participation in gel formation. *Blood* **89,** 4196–4203
20. Himanen, J.-P., Schneider, K., Chait, B., and Manning, J. M. (1995) Participation and strength of interaction of lysine 95(β) in the polymerization of hemoglobin S as determined by its site-directed substitution by isoleucine. *J. Biol. Chem.* **270,** 13885–13891
21. Sivaram, M. V. S., Sudha, R., and Roy, R. P. (2001) A role for the α113 (GH1) amino acid residue in the polymerization of sickle hemoglobin. Evaluation of its inhibitory strength and interaction linkage with two fiber contact sites (α16/23) located in the AB region of the α-chain. *J. Biol. Chem.* **276,** 18209–18215
22. Ho, C., Willis, B. F., Shen, T. J., Dazhen, N. T., Sun, D. P., Tam, M. F., Suzuka, S. M., Fabry, M. E., and Nagel, R. L. (1996) Roles of α114 and β87 amino acid residues in the polymerization of hemoglobin S: Implications for gene therapy. *J. Mol. Biol.* **263,** 475–485
23. Srinivasulu, S., Perumalsamy, K., Upadhya, R., Manjula, B. N., Feiring, S., Alami, R., Bouhassira, E., Fabry, M. E., Nagel, R. L., and Acharya, A. S. (2006) Pair-wise interactions of polymerization inhibitory contact site mutations of hemoglobin-S. *Protein J.* **25,** 503–516
24. Banerjee, S., Mirsamadi, N., Anantharaman, L., Sivaram, M. V., Gupta, R. B., Choudhury, D., and Roy, R. P. (2007) Modification of axial fiber contact residues impact sickle hemoglobin polymerization by perturbing a

network of coupled interactions. *Protein J.* **26,** 445–455
25. Looker, D., Mathews, A. J., Neway, J. O., and Stetler, G. L. (1994) Expression of recombinant human hemoglobin in *Escherichia coli*. *Methods Enzymol.* **231,** 364–374
26. Shen, T. J., Ho, N. T., Simplaceanu, V., Zou, M., Green, B. N., Tam, M. F., and Ho, C. (1993) Production of unmodified human adult hemoglobin in *Escherichia coli*. *Proc. Natl. Acad. Sci. U.S.A.* **90,** 8108–8112
27. Lindstrom, T. R., and Ho, C. (1972) Functional nonequivalence of α and β hemes in human adult hemoglobin. *Proc. Natl. Acad. Sci. U.S.A.* **69,** 1707–1710
28. Tam, M. F., Chen, J., Tam, T. C. S., Tsai, C. H., Shen, T. J., Simplaceanu, V., Feinstein, T. N., Barrick, D., and Ho, C. (2005) Enhanced inhibition of polymerization of sickle cell hemoglobin in the presence of recombinant mutants of human fetal hemoglobin with substitutions at position 43 in the γ-chain. *Biochemistry* **44,** 12188–12195
29. Hayashi, A., Suzuki, T., and Shin, M. (1973) An enzymic reduction system for metmyoglobin and methemoglobin, and its application to functional studies of oxygen carriers. *Biochim. Biophys. Acta* **310,** 309–316
30. Adachi, K., and Asakura, T. (1979) Nucleation-controlled aggregation of deoxyhemoglobin S. Possible difference in the size of nuclei in different phosphate concentrations. *J. Biol. Chem.* **254,** 7765–7771
31. Tam, M. F., Rice, N. W., Maillett, D. H., Simplaceanu, V., Ho, N. T., Tam, T. C., Shen, T. J., and Ho, C. (2013) Autoxidation and oxygen binding properties of recombinant hemoglobins with substitutions at the αVal-62 or βVal-67 position of the distal heme pocket. *J. Biol. Chem.* **288,** 25512–25521
32. Plateau, P., and Gueron, M. (1982) Exchangeable proton NMR without base-line distortion, using new strong-pulse sequences. *J. Am. Chem. Soc.* **104,** 7310–7311
33. Dickerson, R. E., and Geis, I. (1983) *Hemoglobin: Structure, Function, Evolution, and Pathology*, pp. 19–61, Benjamin/Cummings, Menlo Park, CA
34. Wyman, J., Jr. (1964) Linked functions and reciprocal effects in hemoglobin: a second look. *Adv. Protein Chem.* **19,** 223–286
35. Hofrichter, J., Ross, P. D., and Eaton, W. A. (1974) Kinetics and mechanism of deoxyhemoglobin S gelation: a new approach to understanding sickle cell disease. *Proc. Natl. Acad. Sci. U.S.A.* **71,** 4864–4868
36. Kowalczykowski, S., and Steinhardt, J. (1977) Kinetics of hemoglobin S gelation followed by continuously sensitive low-shear viscosity. *J. Mol. Biol.* **115,** 201–213
37. Chang, C. K., Simplaceanu, V., and Ho, C. (2002) Effects of amino acid substitutions at β131 on the structure and properties of hemoglobin: evidence for communication between $\alpha_1\beta_1$- and $\alpha_1\beta_2$-subunit interfaces. *Biochemistry* **41,** 5644–5655
38. Russu, I. M., Ho, N. T., and Ho, C. (1987) A proton nuclear Overhauser effect investigation of the subunit interfaces in human normal adult hemoglobin. *Biochim. Biophys. Acta* **914,** 40–48
39. Simplaceanu, V., Lukin, J. A., Fang, T. Y., Zou, M., Ho, N. T., and Ho, C. (2000) Chain-selective isotopic labeling for NMR studies of large multimeric proteins: application to hemoglobin. *Biophys. J.* **79,** 1146–1154
40. Fang, T. Y., Simplaceanu, V., Tsai, C. H., Ho, N. T., and Ho, C. (2000) An additional H-bond in the $\alpha_1\beta_2$ interface as the structural basis for the low oxygen affinity and high cooperativity of a novel recombinant hemoglobin (βL105W). *Biochemistry* **39,** 13708–13718
41. Dalvit, C., and Ho, C. (1985) Proton nuclear Overhauser effect investigation of the heme pockets in ligated hemoglobin: conformational differences between oxy and carbonmonoxy forms. *Biochemistry* **24,** 3398–3407
42. Lindstrom, T. R., Norén, I. B. E., Charache, S., Lehmann, H., and Ho, C. (1972) Nuclear magnetic resonance studies of hemoglobins. VII. Tertiary structure around ligand binding site in carbonmonoxyhemoglobin. *Biochemistry* **11,** 1677–1681
43. La Mar, G. N., Nagai, K., Jue, T., Budd, D. L., Gersonde, K., Sick, H., Kagimoto, T., Hayashi, A., and Taketa, F. (1980) Assignment of proximal histidyl imidazole exchangeable proton NMR resonances to individual subunits in hemoglobins A, Boston, Iwate and Milwaukee. *Biochem. Biophys. Res. Commun.* **96,** 1172–1177
44. Takahashi, S., Lin, A. K., and Ho, C. (1980) Proton nuclear magnetic-resonance studies of hemoglobin-M-Boston (α58E7 His → Tyr) and Hemoglobin-M-Milwaukee (β67E11 Val → Glu): spectral assignments of hyperfine-shifted proton resonances and of proximal histidine (E7) NH resonances to the α-chains and β-chains of normal human adult hemoglobin. *Biochemistry* **19,** 5196–5202
45. Ho, C. (1992) Proton nuclear-magnetic-resonance studies on hemoglobin: cooperative interactions and partially ligated intermediates. *Adv. Protein Chem.* **43,** 153–312
46. Fung, L. W. M., and Ho, C. (1975) Proton nuclear magnetic-resonance study of quaternary structure of human hemoglobins in water. *Biochemistry* **14,** 2526–2535
47. Ishimori, K., Imai, K., Miyazaki, G., Kitagawa, T., Wada, Y., Morimoto, H., and Morishima, I. (1992) Site-directed mutagenesis in hemoglobin: functional and structural role of inter- and intrasubunit hydrogen bonds as studied with 37β and 145β mutations. *Biochemistry* **31,** 3256–3264
48. Perutz, M. F., and Mitchison, J. M. (1950) State of haemoglobin in sickle-cell anaemia. *Nature* **166,** 677–679
49. Baudin-Chich, V., Pagnier, J., Marden, M., Bohn, B., Lacaze, N., Kister, J., Schaad, O., Edelstein, S. J., and Poyart, C. (1990) Enhanced polymerization of recombinant human deoxyhemoglobin β6 Glu → Ile. *Proc. Natl. Acad. Sci. U.S.A.* **87,** 1845–1849
50. Patskovska, L. N., Patskovsky, Y. V., Almo, S. C., and Hirsch, R. E. (2005) COHbC and COHbS crystallize in the R2 quaternary state at neutral pH in the presence of PEG 4000. *Acta Crystallogr. D Biol. Crystallogr.* **61,** 566–573
51. Wellems, T. E., Vassar, R. J., and Josephs, R. (1981) Polymorphic assemblies of double strands of sickle cell hemoglobin. Manifold pathways of deoxyhemoglobin S crystallization. *J. Mol. Biol.* **153,** 1011–1026
52. Russu, I. M., and Ho, C. (1980) Proton longitudinal relaxation investigation of histidyl residues of normal human adult and sickle deoxyhemoglobin: evidence for the existence of pre-gelation aggregates in sickle deoxyhemoglobin solutions. *Proc. Natl. Acad. Sci. U.S.A.* **77,** 6577–6581
53. Nagel, R. L., Bookchin, R. M., Johnson, J., Labie, D., Wajcman, H., Isaac-Sodeye, W. A., Honig, G. R., Schilirò, G., Crookston, J. H., and Matsutomo, K. (1979) Structural bases of the inhibitory effects of hemoglobin F and hemoglobin A_2 on the polymerization of hemoglobin S. *Proc. Natl. Acad. Sci. U.S.A.* **76,** 670–672
54. Acharya, A. S., and Seetharam, R. (1985) Reactivity of Glu-22(β) of hemoglobin S for amidation with glucosamine. *Biochemistry* **24,** 4885–4890
55. Rhoda, M. D., Blouquit, Y., Caburi-Martin, J., Monplaisir, N., Galacteros, F., Garel, M. C., and Rosa, J. (1984) Effects of the α20 mutation on the polymerization of Hb S. *Biochim. Biophys. Acta* **786,** 62–66
56. Bookchin, R. M., Balazs, T., Wang, Z., Josephs, R., and Lew, V. L. (1999) Polymer structure and solubility of deoxyhemoglobin S in the presence of high concentrations of volume-excluding 70-kDa dextran: effect of non-S hemoglobins and inhibitors. *J. Biol. Chem.* **274,** 6689–6697
57. Yuan, Y., Tam, M. F., Simplaceanu, V., and Ho, C. (2015) New look at hemoglobin allostery. *Chem. Rev.* **115,** 1702–1724
58. Adachi, K., Pang, J., Reddy, L. R., Bradley, L. E., Chen, Q., Trifillis, P., Schwartz, E., and Surrey, S. (1996) Polymerization of three hemoglobin A_2 variants containing $Val^{\delta 6}$ and inhibition of hemoglobin S polymerization by hemoglobin A_2. *J. Biol. Chem.* **271,** 24557–24563
59. Adachi, K., Konitzer, P., Kim, J., Welch, N., and Surrey, S. (1993) Effects of β6 aromatic amino acids on polymerization and solubility of recombinant hemoglobins made in yeast. *J. Biol. Chem.* **268,** 21650–21656
60. Cao, Z., Liao, D., Mirchev, R., Martin de Llano, J. J., Himanen, J. P., Manning, J. M., and Ferrone, F. A. (1997) Nucleation and polymerization of sickle hemoglobin with Leu β88 substituted by Ala. *J. Mol. Biol.* **265,** 580–589
61. Reddy, L. R., Reddy, K. S., Surrey, S., and Adachi, K. (1996) Role of hydrophobic amino acids at β85 and β88 in stabilizing F helix conformation of hemoglobin S. *J. Biol. Chem.* **271,** 24564–24568
62. McCune, S. L., Reilly, M. P., Chomo, M. J., Asakura, T., and Townes, T. M. (1994) Recombinant human hemoglobins designed for gene therapy of sickle cell disease. *Proc. Natl. Acad. Sci. U.S.A.* **91,** 9852–9856
63. Srinivasulu, S., Acharya, A. S., Prabhakaran, M., Fabry, M. E., Alami, R., Fiering, S. N., Bouhasirra, E. E., and Nagel, R. L. (2007) HbS-Savaria: the anti-polymerization effect of a single mutation in human α-chains. *Protein J.* **26,** 523–532